Clays and Clay Minerals, Vol. 41, No. 6, 738–744, 1993.

RIETVELD REFINEMENT OF THE KAOLINITE STRUCTURE AT 1.5 K

DAVID L. BISH

Earth and Environmental Sciences Division, Los Alamos National Laboratory
Los Alamos, New Mexico 87545

Abstract—The crystal structure of Keokuk kaolinite, including all H atoms, was refined in space group *C1* using low-temperature (1.5 K) neutron powder diffraction data (λ = 1.9102 Å) and Rietveld refinement/difference-Fourier methods to R_{wp} = 1.78%, reduced χ^2 = 3.32. Unit-cell parameters are: a = 5.1535(3) Å, b = 8.9419(5) Å, c = 7.3906(4) Å, α = 91.926(2)°, β = 105.046(2)°, γ = 89.797(2)°, and V = 328.70(5) Å^3. Unit-cell parameters show that most of the thermal contraction occurred along the [001] direction, apparently due to a decrease in the interlayer distance. The non-H structure is very similar to published *C1* structures, considering the low temperature of data collection, but the H atom positions are distinct. The inner OH group is essentially in the plane of the layers, and the inner-surface OH groups make angles of 60°–73° with the (001) plane. Difference-Fourier maps show minor anisotropy of the inner-OH group in the [001] direction, but the inner-surface OH groups appear to have their largest vibrational (or positional disorder) component parallel to the layers. Although no data indicate a split position of any of the H sites in kaolinite, there is support for limited *random* positional disorder of the H atoms. However, these data provided no support for a space group symmetry lower than *C1*.

Key Words—Crystal structure, H positions, Kaolinite, Low temperature, Neutron powder diffraction, Rietveld refinement.

INTRODUCTION

Since Pauling first outlined the crystal structure of kaolinite over sixty years ago (Pauling, 1930), many studies have been conducted to clarify the details of its structure. The first comprehensive study (Brindley and Robinson, 1946) used X-ray powder diffraction data to locate the non-H atoms in kaolinite. Since then, little additional information has been obtained on the non-H structure, but there remains little agreement on the locations of the H atoms. H-atom orientations were originally inferred from infrared spectroscopic data, and positions were later modeled by Giese and Datta (1973) and Giese (1982) using electrostatic energy calculations. More recently, Suitch and Young (1983) and Young and Hewat (1988) refined H-atom positions using neutron powder diffraction data but assuming the space group of *P1*. H-atom positions were determined also in the Rietveld study of the St. Austell kaolinite (Adams, 1983), but the diffraction pattern exhibited two-dimensional diffraction effects that are not modeled by the Rietveld method. In addition, the St. Austell material consists of at least two variants of kaolinite (Plançon *et al.*, 1989). Consequently, there is uncertainty in the derived atomic positions. Because of the lack of agreement in the literature concerning the H positions, a Rietveld refinement of the kaolinite structure was undertaken in space group *C1* using low-temperature (1.5 K) neutron powder diffraction data kindly provided by Professor R. Young and A. Hewat.

THE SPACE GROUP OF KAOLINITE

A crystal structure refinement requires the determination of the space group consistent with available observations. Although most investigators have accepted space group *C1*, Suitch and Young (1983) and Young and Hewat (1988) assumed space group *P1*. This assumption requires twice the number of independent atoms in the asymmetric unit by allowing crystallographically identical atoms in *C1* to occupy nonequivalent sites in *P1*. Although Young and coworkers concluded that the non-H portion of the structure largely obeys *C*-centering, the important result of the *P1* refinements was that OH groups that are equivalent in *C1* exhibited two different orientations in *P1*. These orientations have important effects, for example, in vibrational spectroscopy (e.g., Brindley *et al.*, 1986; Johnston *et al.*, 1990), the calculation of X-ray powder diffraction patterns (e.g., Bookin *et al.*, 1989; Plancon *et al.*, 1989), and electrostatic modeling of the structure (e.g., Abbott, 1989; Guthrie and Bish, 1991). Thus, it is crucial to examine the available evidence concerning the true space group.

Differentiation between a *P1* and *C1* space group involves the determination that $h + k$ = odd diffraction data are systematically absent for all *hkl* reflections, which indicates a *C*-centered lattice. The search for reflections violating *C*-centering is potentially complicated by the fact that the violating reflections in kaolinite have been postulated to arise primarily from the H atoms (Suitch and Young, 1983; Young and Hewat, 1988), which do not contribute greatly to X-ray diffraction intensities. However, it is possible that deviations in the Young and Hewat (1988) model from a *C*-centered lattice may also be due to small distortions of the heavier atoms. To test this possibility, an X-ray powder diffraction pattern was calculated for CuKα radiation using POWD10 (Smith *et al.*, 1983)

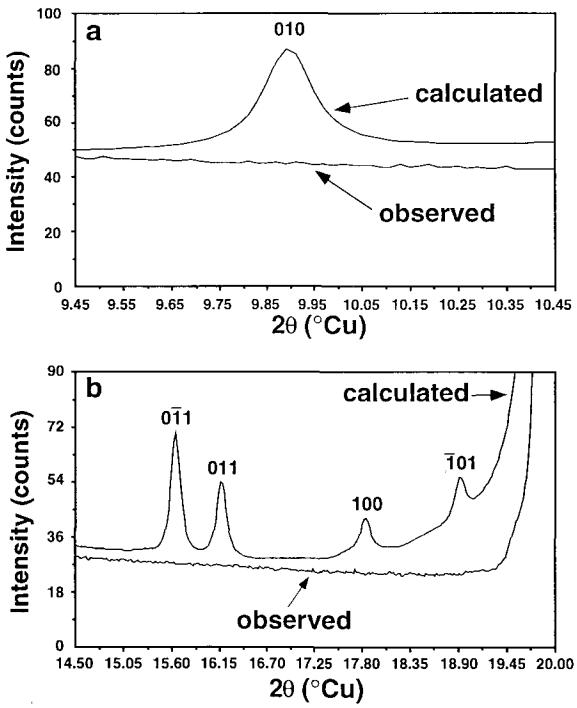

Figure 1. Observed diffraction patterns for Keokuk kaolinite in the vicinity of a) *C1*-violating reflection 010 at 9.90° 2θ, I_{calc} = 1.4; and b) *C1*-violating reflections 0$\bar{1}$1 at 15.63°, I_{calc} = 1.6; 011 at 16.16°, I_{calc} = 1.0; 100 at 17.82°, I_{calc} = 0.4; and $\bar{1}$01 at 18.91° 2θ, I_{calc} = 0.5. Observed patterns were obtained using an automated Siemens D-500 θ-θ diffractometer with a Kevex solid-state Si detector and count times of 378 s/0.02° 2-θ step. Superimposed diffraction patterns were calculated with POWD10 (Smith *et al.*, 1983) using the Young and Hewat (1988) *P1* model with a maximum relative intensity of 100. The full scale of the two patterns was matched using the 20.4° 2θ peak, and the background of the calculated patterns was offset to approximate that found in the experimental pattern. The standard deviation of the counts at each step in the pattern is related to the square root of the total counts accumulated, i.e., $\sqrt{378}$* cps. Thus 1σ at the position of the 9.9° peak is ~0.35 cps.

and the Young and Hewat (1988) kaolinite structure model. The results of this calculation reveal the presence of several weak but statistically significant reflections violating *C*-centering (Figure 1), demonstrating that the non-H portion of the Young and Hewat (1988) model does indeed contribute to the violation of *C*-centering. The violating reflections include (relative integrated intensities in parentheses) 010 (1), 0$\bar{1}$1 (1), 101 (1), 0$\bar{1}$2 (3), $\bar{1}$21 (1), $\bar{1}$23 (2), 1$\bar{2}$3 (1), and $\bar{1}$51 (1). Although many of these reflections should be readily visible in measured kaolinite powder diffraction patterns, the experimental X-ray powder diffraction pattern of Keokuk kaolinite in Figure 1 shows no statistically significant intensity above background at the calculated positions of these reflections, indicating that kaolinite has space group *C1*. Furthermore, the observed neutron diffraction data used by Young and

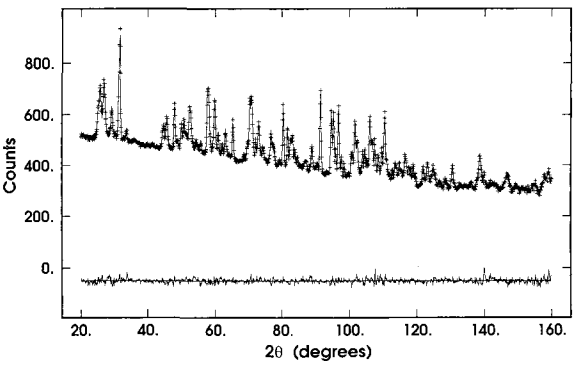

Figure 2. Observed (pluses) and calculated (solid line) neutron powder diffraction pattern for kaolinite. The bottom curve is the difference between observed and calculated profiles. The observed pattern illustrates the 1.5 K data described in the text, and the calculated pattern reflects the final *C1* model.

Hewat (1988) also do not show evidence of reflections violating *C*-centering (Figure 2) as all observed peaks are accounted for by the *C1* model. Young (1988) stated that visual inspection of the neutron powder diffraction pattern of Keokuk kaolinite could not detect violating reflections due to peak overlap and low intensities, but the data in Figure 1 suggest otherwise. Such violations, if present, should be readily detected using diffraction data. Also noteworthy is that the extraction of observed intensities in Rietveld refinement is somewhat model dependent, particularly for low-intensity reflections; and therefore, a reasonable fit in a lower space group is no substitute for visual identification of violating reflections.

Spectroscopic and diffraction data are also consistent with the presence of *C*-centering in kaolinite. Brindley *et al.* (1986) concluded that the *P1* structure of kaolinite was incompatible with the observed character of the ν_4 band (inner-OH vibration) in infrared spectra of a variety of kaolinites. The *P1* structure, with two distinct inner-OH group orientations, should yield an infrared spectrum with a doubled or broadened ν_4 band with some temperature dependence arising from the different environments occupied by the two inner-hydroxyl protons. Instead, they consistently observed only a single sharp ν_4 band, and other investigators (e.g., Prost *et al.*, 1989) have seen little temperature dependence for this absorption band. Thompson and Withers (1987) and Thompson *et al.* (1989) presented convergent-beam electron diffraction patterns for kaolinite that showed the absence of reflections violating *C*-centering. Their calculations for the Young and Hewat (1988) model showed that intensity should have been observable for reflections violating *C*-centering. They concluded that the non-H portion of the structure obeys *C*-centering and that it is probable that the H atoms do not violate *C*-centering.

Finally, the Suitch and Young (1983) and the Young

https://doi.org/10.1346/CCMN.1993.0410613 Published online by Cambridge University Press

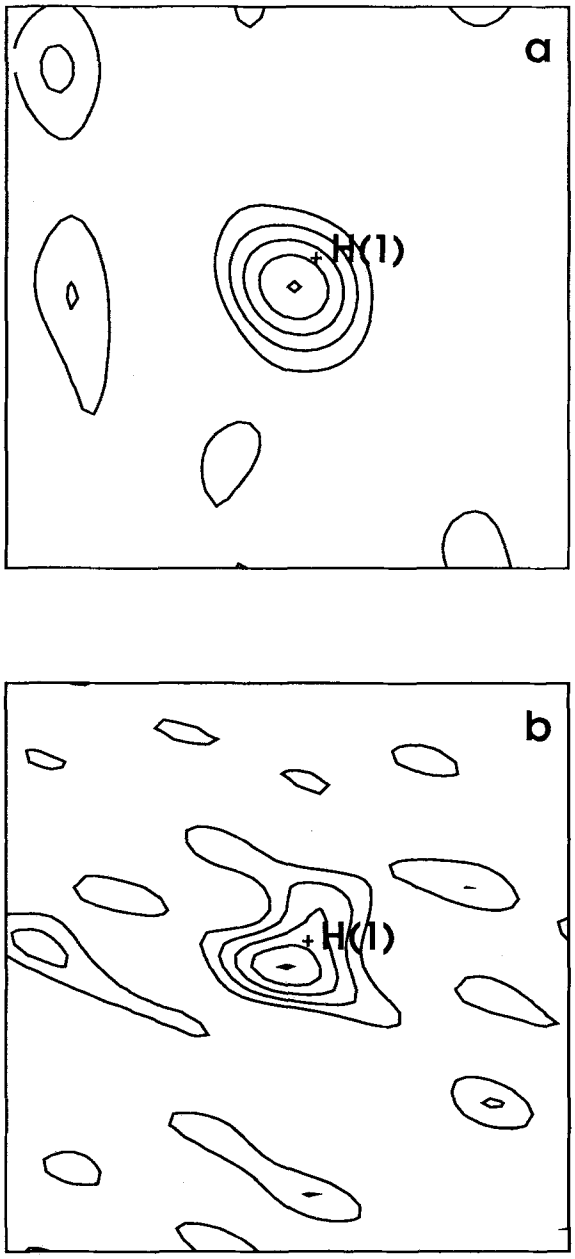

Figure 3. Difference-Fourier map in the region of the inner-hydroxyl proton (z = 0.293, A: x horizontal, y vertical; B: x horizontal, z vertical). Contours are drawn at −0.25, −0.20, −0.15, −0.10, and −0.05. Plus (+) symbol represents the final refined position of H1.

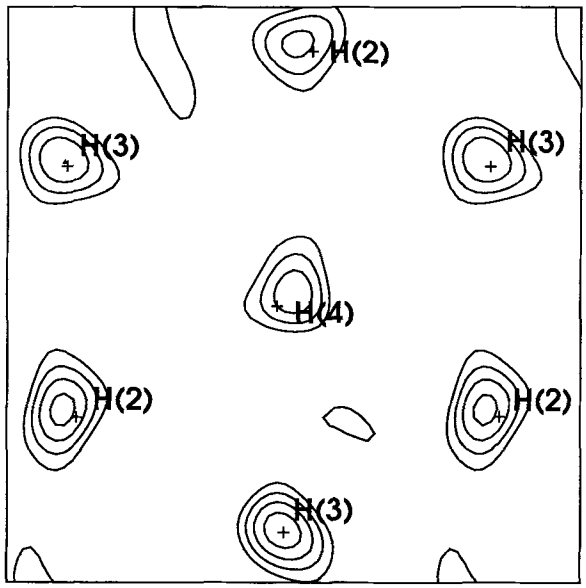

Figure 4. Difference-Fourier map in the interlayer region (z = 0.751, x horizontal, y vertical) showing the positions of the interlayer hydroxyl protons. Contours are drawn at −0.25, −0.20, −0.15, −0.10, and −0.05. Plus (+) symbols represent the final refined positions of each interlayer H atom.

and Hewat (1988) models of kaolinite may represent false-minimum structures. Bish and Von Dreele (1989) demonstrated that attempts to refine the structure of kaolinite using their X-ray powder diffraction data and either the Suitch and Young (1983) or the Young and Hewat (1988) models as starting parameters always resulted in refined structure models with unreasonable bond distances. These distances are similar to those published by Young and coworkers. The Si-O, Al-O, and O-H bond lengths obtained by Suitch and Young (1983) and Young and Hewat (1988) are unusual and in some cases fall far outside accepted ranges. However, with a distance least-squares (DLS) structure of kaolinite as a starting model (Bish and Von Dreele, 1989), the resulting refined structure was crystal-chemically reasonable and the weighted profile residuals were significantly lower (18.0% for the *P1* starting model *vs.* 12.3% with the DLS starting model). Baur and Tillmanns (1986) suggested that these aspects are characteristic of refinements conducted using unnecessarily low symmetry. Thus, the refinement and partial structure solution of kaolinite were conducted using space group *C1*; there is no substantive evidence for lower space group symmetry.

EXPERIMENTAL METHODS

The kaolinite sample (Young and Hewat, 1988) was a composite from several Keokuk, Iowa, geodes. Neutron powder diffraction data (PNKAO86 of Young and Hewat) were obtained using the D1A high-resolution neutron diffractometer at the Institut Laue-Langevin, Grenoble, France, using a wavelength of ~1.91 Å and collecting from 6°–160° 2θ. Although Young and Hewat (1988) were unable to use the data below 42.75° 2θ due to asymmetry in the low-angle reflections, the profile function in the Rietveld refinement program, GSAS (Larson and Von Dreele, 1988), used here allowed the use of data from 20°–160° 2θ. Initial attempts to refine the structure using both neutron and room-tempera-

ture X-ray data were unsuccessful, and it appeared that the neutron data were collected at low temperature. The low-temperature conditions for the neutron data were later confirmed (1.5 K, A. Hewat, personal communication), and a joint X-ray-neutron refinement could not be performed. No chemical analysis of the kaolinite was made, and the structure refinement assumed ideal composition. The non-H-atom positions determined by Bish and Von Dreele (1989) were used as the starting model in space group *C1*. The convolution function described by Von Dreele *et al.* (1982), which considers anisotropic broadening, was used to model the experimental profiles, and a six-term Fourier series modeled the backgrounds.

Initially, refinement of unit-cell parameters, scale factor, instrument zero point, and profile parameters was performed, with the positions of the non-H atoms fixed and no H atoms included. In the absence of the instrumental profile parameters, no absolute information on strain or crystallite size broadening was obtained. As Bish and Von Dreele (1989) showed, there is a small amount of dickite (<4 wt. %) in Keokuk kaolinite, and only the dickite scale factor and unit-cell parameters were independently varied; atomic positions were fixed at the values given by Joswig and Drits (1986), with the z coordinate of the Si1 atom changed to 0.0407 to correct a typographical error; and profile and preferred orientation parameters were constrained to equal those for kaolinite throughout the refinement. Difference-Fourier maps were then calculated to locate the H atoms. The Fourier maps (Figures 3 and 4) indicated four significant regions of negative neutron density, with other minor negative and positive regions. Four apparent H atoms were added to the asymmetric unit, and refinement proceeded with the application of "soft" distance constraints and all atomic positions varied. A total of 57 soft constraints was used, eight tetrahedral distances of 1.61 Å, 12 octahedral distances of 1.91 Å, four O–H distances of 0.98 Å, and a variety of O–O distances. The soft constraints were weighted so that they made up 9.5% of the total minimization function [$M = \Sigma W_i(y_o - y_i)^2$]. The use of difference-Fourier maps to locate H atoms based on a model that is largely correct is preferable to the approach of Young and coworkers, who used electrostatic modeling to provide starting H atom positions. The present procedure made *no* assumptions regarding the positions of the H atoms.

The difference-Fourier maps provided no evidence of a split, dual position for H1, the inner-hydroxyl proton, although anisotropy was evident in the x–z maps for H1 (Figure 3). The primary neutron density occurred at $z \sim 0.321$, with minor density lobes at $z \sim 0.256$ and $z \sim 0.390$. This anisotropy was subsequently modeled in two ways: 1) assuming anisotropic displacement of one H, and 2) assuming positional disorder of three distinct sites, a central one and two side lobes, constraining the total occupancy of all three sites to 1.0. The results of refinements assuming anisotropic displacement of the inner-hydroxyl proton were superior to those using discrete positional disorder, and the latter model failed to converge.

Anisotropic profile coefficients and the March function preferred orientation correction (Dollase, 1986), using [001] as the special direction, were varied in the final stages of refinement. The preferred orientation correction refined to a value of 1.019(4), reflecting the near lack of preferred orientation in the powder sample.

Subsequently, isotropic displacement parameters were varied for groups of similar atoms (O atoms, hydroxyl O atoms, H atoms, Al atoms, and Si atoms grouped together). These parameters were followed by an absorption correction based on the ideal chemistry and an assumed packing density of 50%. A full isotropic refinement (2856 observations, including 57 soft constraints), with different displacement parameters for each H atom, yielded an overall $R_{wp} = 1.94\%$ and a reduced $\chi^2 = 3.87$ (82 variables). Final cycles with anisotropic H atoms (overall $R_{wp} = 1.78\%$, reduced $\chi^2 = 3.32$, 102 variables) revealed significant anisotropy, particularly for H1, but some of the H anisotropic displacement parameters were non positive-definite, possibly due to errors in the absorption correction, which was not allowed to vary. Because of the highly absorbing nature of fully hydrogenated kaolinite in a neutron beam, diffraction probably occurred primarily from near the surface of the sample container, giving rise to an incomplete absorption correction. Final atomic positions from the anisotropic-H refinement, using soft constraints, and isotropic displacement parameters for the non-H atoms are given in Table 1; H-displacement parameters are from the isotropic refinement. Figure 2 shows the observed and calculated diffraction data. Table 2 lists the anisotropic displacement parameters for H. Final unit-cell parameters from the anisotropic refinement were: $a = 5.1535(3)$ Å, $b = 8.9419(5)$ Å, $c = 7.3906(4)$ Å, $\alpha = 91.926(2)°$, $\beta = 105.046(2)°$, $\gamma = 89.797(2)°$, and $V = 328.70(5)$ Å^3. Refinement (102 variables) without soft constraints yielded an $R_{wp} = 1.65\%$ and a reduced $\chi^2 = 2.64$. A final difference-Fourier calculation yielded relatively flat maps, with random very small peaks above and below 0.0.

RESULTS AND DISCUSSION

The resulting non-H structure in space group *C1* (Table 1) is very similar to those previously published, considering the low-temperature data (and the associated thermal contraction). In general, the estimated standard deviations are smaller than other published values. Si–O and Al–O bond lengths (Table 3) are crystal-chemically reasonable, and octahedral shared edges are significantly shortened. Soft constraints had a small

https://doi.org/10.1346/CCMN.1993.0410613 Published online by Cambridge University Press

Table 1. Final atomic parameters for Keokuk kaolinite at 1.5 K.

Atom	*x*	*y*	*z*	U_{iso}(Å²)[1]
Al(1)	0.289(2)[2]	0.4966(7)	0.466(1)	0.040(1)
Al(2)	0.793(2)	0.3288(7)	0.465(1)	0.040(1)
Si(1)	0.989(1)	0.3395(5)	0.0906(9)	0.042(2)
Si(2)	0.507(1)	0.1665(5)	0.0938(9)	0.042(2)
O(1)	0.049(1)	0.3482(7)	0.3168(9)	0.044(1)
O(2)	0.113(2)	0.6599(6)	0.3188(9)	0.044(1)
O(3)	0.0	0.5	0.0	0.044(1)
O(4)	0.204(1)	0.2291(6)	0.030(1)	0.044(1)
O(5)	0.197(1)	0.7641(7)	0.001(1)	0.044(1)
OH(1)	0.050(2)	0.9710(6)	0.325(1)	0.039(1)
OH(2)	0.960(2)	0.1658(6)	0.607(1)	0.039(1)
OH(3)	0.037(2)	0.4726(7)	0.6046(9)	0.039(1)
OH(4)	0.038(2)	0.8582(7)	0.609(1)	0.039(1)
H(1)	0.145(3)	0.0651(1)	0.326(2)	0.073(4)[3]
H(2)	0.063(3)	0.1638(1)	0.739(1)	0.047(3)[3]
H(3)	0.036(3)	0.5057(2)	0.732(1)	0.056(4)[3]
H(4)	0.534(3)	0.3154(2)	0.728(1)	0.049(3)[3]

[1] $U_{iso} = B_{iso}/8\pi^2$.
[2] Values in parentheses are estimated standard deviations in the last place.
[3] H displacement parameters from isotropic refinement.

effect on the apparent accuracy of the bond lengths, as judged by refinements done without the use of constraints. The tetrahedral rotation angle at 1.5 K is 7.3(4)° *vs.* 6.9° for the room-temperature value (Bish and Von Dreele, 1989). Similarly, Bish and Johnston (1993) found that the tetrahedral rotation angle for dickite increased by ~0.5° upon reducing the sample temperature to 12 K.

Effects of temperature

The refined unit-cell parameters show that, as with dickite (Bish and Johnston, 1993), most of the thermal contraction occurred along the *c* axis. Compared with the unit-cell parameters obtained by Bish and Von Dreele (1989) for Keokuk kaolinite at room temperature, *a* decreased by 0.04% and *b* decreased by 0.03%, whereas *c* decreased by 0.19%. The changes in all three parameters are significant at the 3σ level. Comparison with the room-temperature structure (Bish and Von Dreele, 1989) shows that, as with dickite, the decrease along the *c* axis is related primarily to a decrease in the interlayer separation (~0.013 Å), although the average octahedral thickness is slightly smaller at low temperature.

OH orientations

The O–H bond distances in Table 4 are crystal-chemically reasonable, lying between 0.975 and 0.982 Å, although they were undoubtedly affected by the use of soft distance constraints. The interlayer H bonding geometries (Table 4) show that OH(4) is strongly H-bonded, whereas OH(2) is least H-bonded. The H-bonding systematics are consistent with the assignment of OH(2) to the 3696 cm^{-1} band, OH(3) to the 3668 cm^{-1} band, and OH(4) to the 3651 cm^{-1} band in infrared (IR) spectra (c.f., Figure 6 of Johnston *et al.*, 1990). In addition, the significant difference between the hydrogen bond lengths of the three inner-surface OH groups is consistent with the observation of three well-resolved inner-surface OH vibrations in IR spectra. In contrast, the hydrogen bond distances for OH(2) and OH(4) in dickite are sufficiently close that two distinct ν(OH) bands for OH(2) and OH(4) are not resolved in IR spectra. The angle between OH(1) and the (001) plane is <1°, whereas Giese (1982) calculated an angle of 15°. The observed orientations in Table 4 are very close to those modeled by Guthrie and Bish (1991), and the observed OH(1) orientation is close to that modeled by Hess and Saunders (1992).

The anisotropic displacement parameters in Table 2 show that H1 exhibits the largest amount of positional disorder (or thermal motion) perpendicular to the layers, whereas H2, H3, and H4 exhibit the largest amount of positional disorder within the plane of the layers, consistent with the orientation of the OH bonds. Although the magnitudes of the displacement parameters are in error, possibly due to an incomplete absorption correction, the general shapes of the vibrational ellipsoids do approach those obtained by Guthrie and Bish (1991) in their electrostatic minimization calculations. H1 occupies a shallow energy minimum oriented approximately perpendicular to the layers, whereas the inner-surface hydroxyl protons occupy disk-shaped energy minima approximately parallel to the layers.

The split, distinct positions for the inner-hydroxyl protons determined by Suitch and Young (1983) and Young and Hewat (1988) are probably artifacts of refining the structure in an unwarranted low space-group symmetry. Artifacts are common in such refinements (e.g., Baur and Tillmanns, 1986). If split, distinct positions occur, then difference-Fourier maps calculated in space group *C1* should show two partially occupied

Table 2. Anisotropic displacement parameters for H atoms.

Atom	U_{11}(Å²)	U_{22}(Å²)	U_{33}(Å²)	U_{12}(Å²)	U_{13}(Å²)	U_{23}(Å²)
H(1)	0.033(7)	0.050(7)	0.11(1)	0.019(5)	0.033(7)	0.006(7)
H(2)	0.084(8)	0.051(6)	−0.008(6)	−0.011(5)	−0.010(6)	−0.014(4)
H(3)	0.066(8)	0.080(8)	0.028(9)	0.025(7)	0.016(7)	0.003(7)
H(4)	0.067(8)	0.093(9)	−0.024(5)	0.000(6)	−0.006(3)	0.025(5)

https://doi.org/10.1346/CCMN.1993.0410613 Published online by Cambridge University Press

Table 3. Si–O and Al–O bond lengths (Å) for kaolinite.

Si(1)–O(1)	1.618(4)[1]Å	Si(2)–O(2)	1.612(4)Å
–O(3)	1.611(4)	–O(3)	1.617(4)
–O(4)	1.620(4)	–O(4)	1.616(4)
–O(5)	1.619(4)	–O(5)	1.608(4)
	1.617(8)		1.613(8)
Al(1)–O(1)	1.927(6)Å	Al(2)–O(1)	1.931(6)Å
–O(2)	1.930(6)	–O(2)	1.919(6)
–OH(1)	1.913(6)	–OH(1)	1.912(6)
–OH(2)	1.890(6)	–OH(2)	1.896(6)
–OH(3)	1.865(6)	–OH(3)	1.886(6)
–OH(4)	1.915(6)	–OH(4)	1.910(6)
	1.907(15)		1.909(15)

[1] Values in parentheses are estimated standard deviations in the last place(s).

Table 4. Structural parameters for OH groups in kaolinite.

Atom	O–H(Å)	Angle of OH with *b*-axis	Angle of OH with (001) plane	O–H···O(Å)	
OH(1)	0.975(4)[1]	30.39°	0.38°		
OH(2)	0.982(4)	79.71°	73.16°	··O(4)	3.087(6)
OH(3)	0.976(4)	43.13°	68.24°	··O(3)	2.980(7)
OH(4)	0.975(4)	31.10°	60.28°	··O(5)	2.945(7)
	0.977(8)				

[1] Values in parentheses are estimated standard deviations in the last place.

H positions, essentially an average of the *P1* structure. However, this is not the case.

Nevertheless, there are data suggesting that H1 may exhibit some *random* positional disorder. However, because this disorder is non periodic, there is no reduction in space group to *P1*. For example, simple anisotropic vibration or statistical distribution of an H atom will not cause the *C*-centering to be violated unless it occurs in a periodic, non-random fashion. Difference-Fourier maps (Figure 3) and anisotropic displacement parameters (Table 2) show that H1 has its largest component of positional displacement approximately along [001]. Because these data were obtained at 1.5 K, the anisotropic displacement parameters probably reflect positional disorder and not thermal motion. Alternatively, artifacts due to the limitations inherent in calculating difference-Fourier maps during Rietveld refinement may exist. However, both electrostatic energy modeling (Guthrie and Bish, 1991, which indicates a shallow rod-shaped energy minimum oriented approximately parallel to [001] for the H1 atom, and spectroscopic evidence (unpublished, cited by Thompson *et al.*, 1989), showing two inner-OH orientations along [001], support positional disorder. Low-temperature infrared spectra of Keokuk kaolinite (C. Johnston, personal communication) also are consistent with a single, possibly positionally disordered, site for H1. Johnston found that the temperature dependence of the line width for the Keokuk kaolinite inner-OH stretching band is in accord with predictions for statistical occupancy of the H1 atom on multiple sites. Johnston also determined that the inner-OH stretching vibration for Keokuk kaolinite had >90% Lorentzian character. Typically the profile of one non-overlapped band is primarily Lorentzian, whereas the composite profile of two partly overlapped Lorentzian bands is Gaussian. These absorption spectra are, therefore, inconsistent with an H1 atom on *two distinct* sites (thus yielding two distinct OH-stretching vibrations) but are consistent with random positional disorder. Thus, both diffraction and absorption spectroscopic data indicate *long-range* symmetry consistent with space group *C1*. Only methods sensitive to local interactions are capable of detecting the possible statistical occupancy of the H1 atom, and this appears to be a fruitful area for future study.

In summary, this refinement in space group *C1* showed zero intensities for all reflections that might violate *C*-centering. In addition, the refinement converged to a lower agreement factor (R_{wp} = 1.65%, 102 variables, without soft constraints) than that obtained by Young and Hewat (R_{wp} = 2.03%, 116 variables) using the same data in *P1*. Also, the present refinement used neutron data from 20° to 160° 2θ, whereas Young and Hewat (1988) used data starting at 42.75°. In general, an equally good model with more refined variables and/or fewer data will yield a lower agreement factor than one with fewer refined variables or more data. Thus, the lower agreement factor obtained in the present refinement is particularly significant.

ACKNOWLEDGMENTS

I am particularly grateful to Prof. R. Young of the Georgia Institute of Technology for providing his neutron powder diffraction data and for encouraging an independent analysis of the kaolinite structure. C. Johnston, Department of Agronomy, Purdue University, kindly shared his low-temperature infrared spectra for kaolinites. My thanks also go to G. Guthrie, C. Johnston, and S. Guggenheim for helpful comments on the manuscript, to R. Von Dreele for assistance with early stages of the refinement, and to A. Hewat for information on the data collection conditions. This research was supported by the U.S. Department of Energy through contract #W-7405-ENG-36 to Los Alamos National Laboratory.

REFERENCES

Abbott, R. N., Jr. (1989) Kaolinite: Energy calculations bearing on the location of the inner hydrogen atoms: in *Abstracts with Program, 1989 Annual Meeting of the Geological Society of America,* St. Louis, Missouri, p. A43 (abstract).

Adams, J. M. (1983) Hydrogen atom positions in kaolinite by neutron profile refinement: *Clays & Clay Minerals* **31,** 352–356.

Baur, W. H. and Tillmanns, E. (1986) How to avoid unnecessarily low symmetry in crystal structure determinations: *Acta Crystallogr.* **B42,** 95–111.

Bish, D. L. and Johnston, C. T. (1993) Rietveld refinement and Fourier-transform infrared spectroscopic study of the dickite structure at low temperature: *Clays & Clay Minerals* **41,** 297–304.

Bish, D. L. and Von Dreele, R. B. (1989) Rietveld refinement of non-hydrogen atomic positions in kaolinite: *Clays & Clay Minerals* **37,** 289–296.

Bookin, A. S., Drits, V. A., Plançon, A., and Tchoubar, C. (1989) Stacking faults in kaolin-group minerals in the light of real structural features: *Clays & Clay Minerals* **37,** 297–307.

Brindley, G. W., Kao, C.-C., Harrison, J. L., Lipsicas, M., and Raythatha, R. (1986) Relation between structural disorder and other characteristics of kaolinites and dickites: *Clays & Clay Minerals* **34,** 239–249.

Brindley, G. W. and Robinson, K. (1946) The structure of kaolinite: *Mineral. Mag.* **27,** 242–253.

Dollase, W. A. (1986) Correction of intensities for preferred orientation in powder diffractometry: Application of the March model: *J. Appl. Crystallogr.* **19,** 267–272.

Giese Jr., R. F. and Datta, P. (1973) Hydroxyl orientation in kaolinite, dickite, and nacrite: *Amer. Mineral.* **58,** 471–479.

Giese Jr., R. F. (1982) Theoretical studies of the kaolin minerals: Electrostatic calculations: *Bull. Mineral.* **105,** 417–424.

Guthrie, G. D. and Bish, D. L. (1991) Ionic modeling of the hydrogen sites in the kaolin polymorphs: in *Program and Abstracts, 28th Annual Meeting of the Clay Minerals Society,* Houston, Texas, p. 63 (abstract).

Hess, A. C. and Saunders, V. R. (1992) Periodic *ab initio* Hartree-Fock calculations of the low-symmetry mineral kaolinite: *J. Phys. Chem.* **96,** 4367–4374.

Johnston, C. T., Agnew, S. F., and Bish, D. L. (1990) Polarized single-crystal Fourier-transform infrared microscopy of Ouray dickite and Keokuk kaolinite: *Clays & Clay Minerals* **38,** 573–583.

Joswig, W. and Drits, V. A. (1986) The orientation of the hydroxyl groups in dickite by X-ray diffraction: *N. Jb. Miner. Mh.* 19–22.

Larson, A. C. and Von Dreele, R. B. (1988) Generalized structure analysis system: *Los Alamos National Laboratory Rept.* **LAUR 86-748,** 150 pp.

Pauling, L. (1930) The structure of the chlorites: *Proc. Natl. Acad. Sci. U.S.A.* **16,** 578–582.

Plancon, A., Giese, R. F., Jr., Snyder, R., Drits, V. A., and Bookin, A. S. (1989) Stacking faults in the kaolin-group minerals: Defect structures of kaolinite: *Clays & Clay Minerals* **37,** 203–210.

Prost, R., Dameme, A., Huard, E., Driard, J., and Leydecker, J. P. (1989) Infrared study of structural OH in kaolinite, dickite, nacrite, and poorly crystalline kaolinite at 5 to 600 K: *Clays & Clay Minerals* **37,** 464–468.

Smith, D. K., Nichols, M. C., and Zolensky, M. E. (1983) POWD10, A FORTRAN IV program for calculating X-ray powder diffraction patterns: The Pennsylvania State University, University Park, Pennsylvania.

Suitch, P. R. and Young, R. A. (1983) Atom positions in highly ordered kaolinite: *Clays & Clay Minerals* **31,** 357–366.

Thompson, J. G., Fitz Gerald, J. D., and Withers, R. L. (1989) Electron diffraction evidence for C-centering of non-hydrogen atoms in kaolinite: *Clays & Clay Minerals* **37,**563–565.

Thompson, J. G. and Withers, R. L. (1987) A transmission electron microscopy contribution to the structure of kaolinite: *Clays & Clay Minerals* **35,** 237–239.

Von Dreele, R. B., Jorgensen, J. D., and Windsor, C. G. (1982) Rietveld refinement with spallation neutron powder diffraction data: *J. Appl. Crystallogr.* **15,** 581–589.

Young, R. A. (1988) Pressing the limits of Rietveld refinement: *Aust. J. Phys.* **41,** 297–310.

Young, R. A. and Hewat, A. W. (1988) Verification of the triclinic crystal structure of kaolinite: *Clays & Clay Minerals* **36,** 225–232.

(Received 16 April 1992; accepted 13 May 1993; Ms. 2363)